Journal of Engineering and Technological Sciences

Modal Transformation-based Fault Location in Radial Distribution Networks

Thant Sin Aung* & Wunna Swe

Department of Electrical Power Engineering, Mandalay Technological University, Patheingyi Township, 05071, Myanmar

*Corresponding author: thantsinaungep@gmail.com

Abstract

This paper introduces a technique to estimate fault distance in radial distribution networks based on modal transformation and signal processing. Recorded faulted phase currents are applied to the Karrenbauer model transformation and these model component currents are decomposed into detail coefficients by the use of Daubechies wavelet db6. A fault recorder installed at the terminal of the feeder records the different time delays between the modal components. In order to find the fault distance, the time delay values and the modal component velocity values are applied to the traveling wave theory. This study compared two different conditions: not using modal transformation and using modal transformation. When using modal transformation, three different coefficient levels were used to estimate the fault distance: detail coefficient level 1 (D1), the combination of detail coefficient level 1+2 (D1+2), and the combination of detail coefficient level 1+2+3 (D1+2+3). Different fault types with different fault locations were created in MATLAB simulation.

Keywords: *Daubechies wavelet (db6); detail coefficient; Karrenbauer transformation; traveling wave theory; wavelet transform.*

Introduction

Nowadays, distribution systems comprise multiple feeders that provide electrical power to the end user. The continuous supply of power to the end user is a major task for the electric supply authorities. During a fault in the distribution feeder, the associated feeder breaker trips, which is called overcurrent earth fault or earth fault. In such a case, the operation manager will try to close the breaker by one trial testing. If this fails, a lineman will check the whole distribution line using visual inspection. When a fault point is identified by visual inspection, a maintenance technician from the electric supply authorities will repair the line. The duration of power outage for the end user depends on the duration of the visual inspection and the severity of the fault. If the fault point can be correctly identified without visual inspection along the distribution line, the duration of power outage can be reduced to a minimum.

Various methods are employed to find the location of faults in both transmission and distribution systems. Iterative estimation of load and fault current in each section of a line is used to identify faults in the efficient location algorithm and diagnosis scheme that was proposed in [1]. A unique fault location technique useful for multi-terminal transmission networks applying a support impedance and traveling wave theory-based technique was developed in [2]. Frequency spectrum components of fault-generated traveling waves were adopted to obtain an accurate and useful method for fault area estimation and fault distance determination in distribution systems [3]. An innovative typical fault location technique for untransposed distribution lines using sparse wide-area calculation was introduced in [4], which is also relevant for transposed lines. A scheme for fault location in distribution systems applying network topology facts and circuit breaker reclosure-generating traveling waves was presented in [5]. The S-transform was used for fault allocation in distribution grids and associated systems (with overhead and underground cable configuration) in [6].

The method presented in [7] utilizes harmonic decomposition of the leakage current for the purpose of analyzing the condition of line insulation, employing a neural network to identify the fault location. By using this method,

ISSN: 2337-5779

DOI: 10.5614/j.eng.technol.sci.2023.55.2.2

DOI: 10.5614/j.eng.technol.sci.2023.55.2.2

it is possible to detect imperfections in the transmission line before any faults occur, which in turn enables predictive maintenance. Reference [8] introduces a novel fault location algorithm for double-circuit series compensated lines that relies on synchronized phasor measurements. The algorithm proposed in [8] does not rely on a model of the series compensation device, thus eliminating errors resulting from such modeling. A technique for fault location in distribution systems is presented in [9], which relies on the frequency spectrum components of the traveling waves generated by faults. This technique involves constructing an offline database and comparing the data obtained from analyzing the fault-generated voltage with information in the database. Signal processing techniques can be utilized to analyze the waveforms of the electrical signals that are generated during a fault in a power system. By analyzing the waveform data, it is possible to extract information about the characteristics of the fault, such as its location and distance from the monitoring equipment. In [10-12], the detail coefficients obtained from wavelet transforms were utilized to identify both the location and the section of the fault. However, this technique needs special devices such as a global positioning system (GPS) clock, a tapped changer, and fault transient detectors.

To overcome fault location problems, this paper presents a new modal transformation of faulted phase currents combined with wavelet transform. Modal transformation is used to remove the mutual effects of the line conductors and obtain the pure transient nature of the faulted currents. The proposed algorithm utilizes faulted current signals from three-phase transients, which are then split into detail coefficient levels using Daubechies wavelet transform db6. The detail coefficient values are then used to obtain the time delay values, which are applied to the traveling wave theory. Fault distance is calculated with two methods to achieve the best accuracy. The first method utilizes the faulted current signals processed using signal processing techniques, without applying modal transformation. The second method utilizes the faulted current signals that are applied to the modal transformation before the signal processing techniques are applied.

This paper is organized as follows: Section 2 describes the proposed methodology, Section 3 describes the Karrenbauer transformation, Section 4 describes the Daubechies wavelet, Section 5 describes the time delay values of the detail coefficients, Section 6 describes the travelling wave theory, Section 7 describes the case selection and data collection, and Section 8 shows the simulation results and analysis. The conclusion in Section 9 closes the paper.

Proposed Methodology

When a fault occurs in a radial distribution system, the impedance of the line conductor drops significantly, resulting in a large faulted phase current flow through the fault location. As a result, the current waveform experiences more significant distortions than the voltage waveform. The proposed methodology relies on fault current data because the transient nature of the faulted phase current provides a more precise basis for extracting the relevant signal properties necessary for fault location. These faulted phase currents are needed to transform the modal components because of the transposition arrangement. The transposition setup of the modal components is used to reduce the mutual effects of inductive coupling of the line and to prevent interference from other power lines. These modal components are applied to a Daubechies wavelet with the order of 6 (db6). The signals are further sub-divided into approximation coefficients and detail coefficients by multi-level decomposition. For power system faults, detail coefficients are normally used to remove the low frequency signal. The proposed methodology uses three types of detail coefficients: level 1 (D1), the combination of level 1+2 (D1+2), and the combination of level 1+2+3 (D1+2+3). It chooses the highest accuracy of the detail coefficient level for the allocation of faults. The time delay is based on the multiplication of sampling time by arrival time of the zero modal component and the line modal component.

The aerial mode velocity is the velocity at which an electromagnetic wave propagates along the length of a distribution line. The term 'zero mode velocity' refers to the velocity that applies to modal transformations and is used to obtain zero mode signals from transient conditions. The aerial mode and the zero mode of the traveling wave velocity are obtained from the associated inductance and capacitance of the distribution line parameters. In order to obtain the exact location of fault points by the proposed algorithm, the traveling waves theory is applied in the final stage. Figure 1 shows the overall fault location algorithm for the proposed methodology.

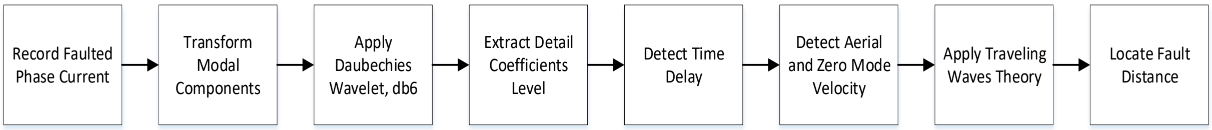

Figure 1 Overall algorithm for proposed methodology.

Karrenbauer Transformation

Radial distribution systems are characterized by non-symmetrical conductors with the effect of capacitance and inductance, complicated topological structure, multiple feeders with different loads, and in the style of an untransposed system. To avoid the effect of capacitance and inductance in the distribution system, the conductors are kept in a transposed position. In a transposed power system, where the transmission lines are modeled as pi-equivalent circuits, modal transformation matrices can be used to analyze the dynamic behavior of the system under different operating conditions, such as changes in load or generation. The transformation matrices can be computed using the system's dynamic matrix, which takes into account the system's inherent damping and the effects of external damping devices such as power system stabilizers. When asymmetrical faults and loads occur in a radial distribution system, the current and voltage are in a transient condition and the Karrenbauer transformation can be applied to obtain α-model, β-model, γ-model and 0-model signals from this transient condition. The use of modal transformation matrices for power systems provides a powerful tool for analyzing the system's dynamic behavior and designing control strategies to maintain stable and reliable operation.

Depending on the fault distance, the modal components will pass through at different speeds along the faulted line. In the proposed methodology, only the phase currents are applied to the Karrenbauer transformation matrix. Eqs. (1) to (4) show the modal components from phase to phase.

$$\mathrm{I}_0 = \frac{1}{3}[\mathrm{I}_a + \mathrm{I}_b + \mathrm{I}_c] \tag{1}$$

$$\mathrm{I}_\alpha = \frac{1}{3}[\mathrm{I}_a - \mathrm{I}_b + 0] \tag{2}$$

$$\mathrm{I}_\beta = \frac{1}{3}[\mathrm{I}_a + 0 - \mathrm{I}_c] \tag{3}$$

$$\mathrm{I}_\gamma = \frac{1}{3}[0 + \mathrm{I}_b - \mathrm{I}_c] \tag{4}$$

where I_0 = zero modal
I_α = line modal between phase A and B
I_β = line modal between phase A and C
I_γ = line modal between phase B and C

Daubechies Wavelet

Wavelet transform is a two-dimensional transformation with an adjustable time and frequency window. There are two main types of wavelet transforms: discrete wavelet transforms (DWT) and continuous wavelet transforms (CWT). CWT is a continuous-time implementation of the wavelet transform, where the signal is decomposed into an infinite number of scales and positions. In [13], the location of seepage and fractures in the subsurface based on self-potential data was determined using CWT. DWT is a digital implementation of the wavelet transform, where the signal is decomposed into a finite number of scales and positions. Ref. [14] proposes a first-order statistical (FOS) texture descriptor based on the discrete wavelet transform (DWT) to identify microscopic images of hardwood species. A proficient numerical integration technique is suggested for estimating the potential energy in pseudo-potential electronic structure calculations utilizing basis sets composed of Daubechies wavelets and scaling functions in [15].

Among the different types of discrete wavelet families, the Daubechies wavelet (db) with order numbers 4 and 6 are widely used in power system applications. In the proposed methodology, db6 is used and a multi-level decomposition method is applied. In multi-level decomposition, approximation coefficients represent the low-

DOI: 10.5614/j.eng.technol.sci.2023.55.2.2

frequency, high-scale components of the signal, whereas the detail coefficients represent the high-frequency, low-scale components. In the proposed methodology, the detail coefficients are used to locate faults because they can capture the high-frequency components of a signal and are therefore better suited to capture the transient behavior associated with faults. Approximation coefficients cannot be used for fault location because they represent the low-frequency component of the signal and are therefore less sensitive to the high-frequency components associated with faults. Figure 2 shows an illustration of multi-level decomposition.

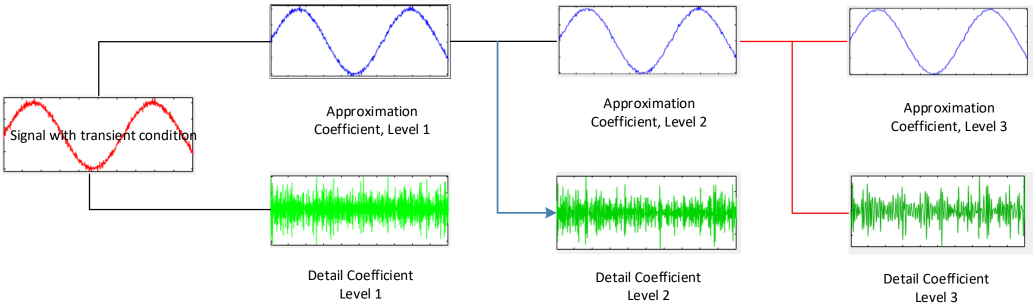

Figure 2 Illustration of multi-level decomposition.

Time Delay Values of Detail Coefficients

In order to obtain modal components, faulted phase currents are applied to the Karrenbauer transform. These modal components of the faulted phase current are passed through db6 wavelets and are decomposed into detail coefficients by the multi-level decomposition method. The time delay between the modal components of the faulted phased current is calculated by Eqs. (5), (6) and (7).

$$T_0 = T_{A_0} \times T_S \tag{5}$$

$$T_1 = T_{A_1} \times T_S \tag{6}$$

$$T_d = T_0 - T_1 \tag{7}$$

where, T_{A_0} = detail coefficient of zero modal component
T_{A_1} = detail coefficient of line model component
T_0 = arrival time of the zero modal component (s)
T_1 = arrival time of the line modal component (s)
T_S = sampling time (s)
T_d = time delay (s)

Travelling Wave Theory

When a fault occurs in a radial distribution system, the transient voltage and current associated with traveling waves propagate towards the sending end and the receiving end of the line. Figure 3 shows that when the fault point is located between busbar 1 and busbar 2, transient traveling waves will travel in both directions over the fault point. Some of the waves are directed towards busbar 2, which is called refraction, and some of the waves are reflected backwards busbar 1, which is called reflection.

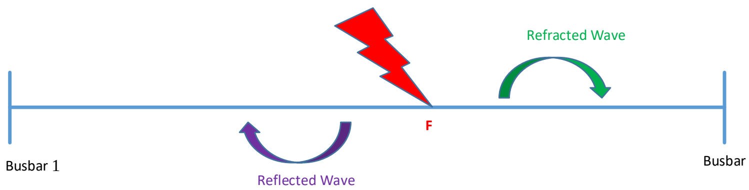

Figure 3 Scheme of a traveling wave system.

The velocity of the traveling wave can be obtained from the inductance and capacitance of the line parameter, which is calculated by Eq. (8):

$$v = \frac{1}{\sqrt{LC}} \quad (8)$$

where, v = velocity of traveling wave (m/s)

L = inductance of the Line (H)

C = capacitance of the Line (F)

The transient wave includes a high-frequency content and the Daubechies wavelet transform can detect the arrival time of a high-frequency occurrence. In the proposed methodology, two approaches of the traveling wave equation are used to find the fault distance. The first approach deals with the direct time detection of the maximum detail coefficients and does not use modal transformation.

$$X = \frac{v \times (t_s - t_r) \times T_s}{2} \quad (9)$$

where; t_s = arrival time at sending end of detail coefficients
t_r = arrival time at receiving end of detail coefficients
T_s = sampling time (s)
v = velocity of traveling wave (m/s)
X = estimated fault distance (m)

The second approach deals with the difference between the arrival time of the line modal and the zero modal components and uses modal transformation calculated by:

$$X = \frac{v_1 v_0 (t_d)}{(v_1 - v_0)} \quad (10)$$

where; t_d = time delay (s)
v_1 = the velocity of the line model component of traveling waves (m/s)
v_0 = the velocity of the zero model component of traveling waves (m/s)
X = the estimated fault distance (m)

The fault distance estimation accuracy (FDEA) can be calculated with Eq. (11):

$$\text{FDEA} = \left(1 - \frac{|\text{Actual Location - Estimated Location}|}{\text{Total Length of Line}}\right) \times 100 \quad (11)$$

Case Selection and Data Collection

The proposed methodology was tested on the 230/33/11 kV (3x100) MVA Myuk Pyin radial distribution network. The network source was taken from the 230kV Aungpinlae substation and this source voltage was stepped down to 33kV/11kV using a 100-MVA stepdown transformer. The network has sixteen feeders of 33 kV and each feeder has a different line length. The fault recorders were installed at the terminal of the 33-kV main busbar and the sampling frequency was 1MHz. According to the monthly fault recorded data, fault occurrence is five times per feeder and the duration of fault recovery can be more than 2 hours, depending on the severity of the fault. A line diagram of the Myuk Pyin radial distribution network is shown in Figure 4.

The proposed network was modeled in a MATLAB Simulation environment. Different feeders with different line lengths were modeled with distributed line parameters and a three-phase load block. The three-phase source block and a three-phase transformer were added in Simulink. The three-phase fault block simulates different fault types. A Power Gui block implements discretization of the electrical system with fixed time steps in the proposed methodology. Figure 5 shows the tested feeder (Ohbo Feeder) in the proposed network. Table 1 describes the main data input into the MATLAB Simulink block.

DOI: 10.5614/j.eng.technol.sci.2023.55.2.2

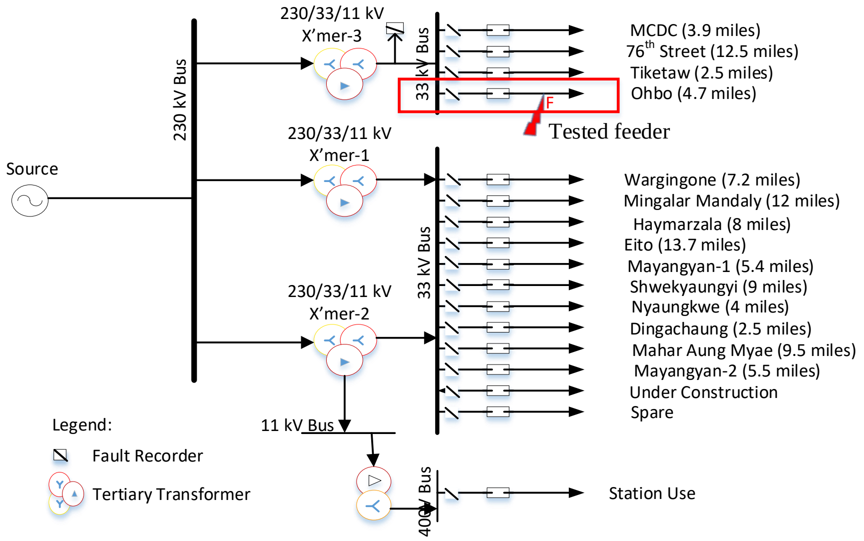

Figure 4 One-line diagram of Myuk Pyin radial distribution system.

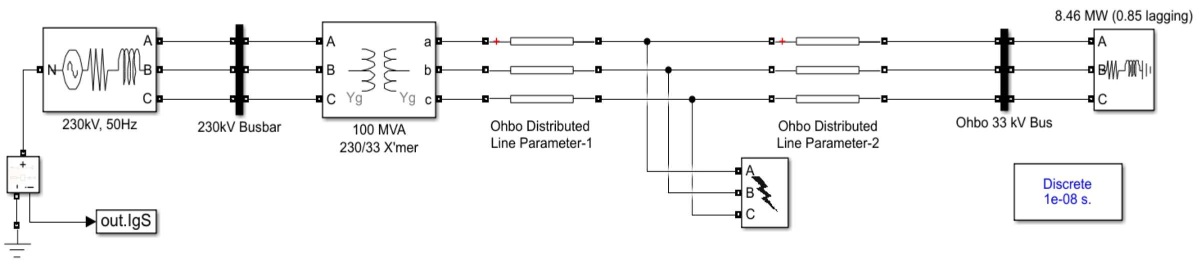

Figure 5 MATLAB model of the tested feeder.

Table 1 Data input of the tested feeder.

Description	Data	Values
Source	Voltage	230kV
	Three-phase short circuit	2604.68×10^{4}
	X/R ratio	1/0.121
Transformer	Nominal power	100×10^{6} W
	Frequency	50Hz
	Winding 1 voltage, winding 2 voltage	230 kV, 33 kV
	Winding resistance	0.135/33 pu, 0.135 pu
Line	Positive sequence and zero sequence resistance	0.1760 ohm/km, 0.2162 ohm/km
	Positive sequence and zero sequence inductance	0.4516 mH/km, 12.368 mH/km
	Positive sequence and zero sequence capacitance	12.74×10^{-9} F/km, 7.751×10^{-9} F/km
	Line length	7.5623 km
Load	Power	8.46 MW

Simulation Results and Analysis

The proposed methodology was tested in two different conditions:

(A) without modal transformation

(B) with Karrenbauer transformation

Without Modal Transformation

In condition (A), different fault types with different faulted phase currents are directly applied to the Daubechies wavelet (db6) without transforming modal components. Detail coefficient level 1 is used in the multi-level decomposition method and records the time of arrival of the detail coefficients at the receiving end and the sending end. The velocity is calculated by the positive sequence inductance and capacitance of the line parameter. Then, the time difference between the receiving end and the sending end of the detail coefficients are used to find the fault distance with Eq. (9). Figure 6 shows the detection of the arrival time from both the receiving end and the sending end by using the wavelet analyzer in MATLAB Toolbox and Table 2 shows the fault distance results for different fault types.

According to the results shown in Table 2, both the phase-to-phase-faults (AB, AC and BC fault) and the three-phase fault (ABC fault) could estimate the fault distance with an accuracy of over 99%. The three-phase to ground fault (ABCG fault) could detect the fault distance with the highest accuracy, at 99.95%. However, other types of ground faults, such as single line to ground faults (AG, BG, CG fault) and double line to ground faults (ABG, BCG and CAG fault), cannot accurately estimate the fault distance in radial distribution networks. This is because faults involving ground conditions are influenced by mutual effects of the line and frequently occur in radial distribution systems. To determine ground fault locations accurately, the mutual effects must be removed by modal transformation.

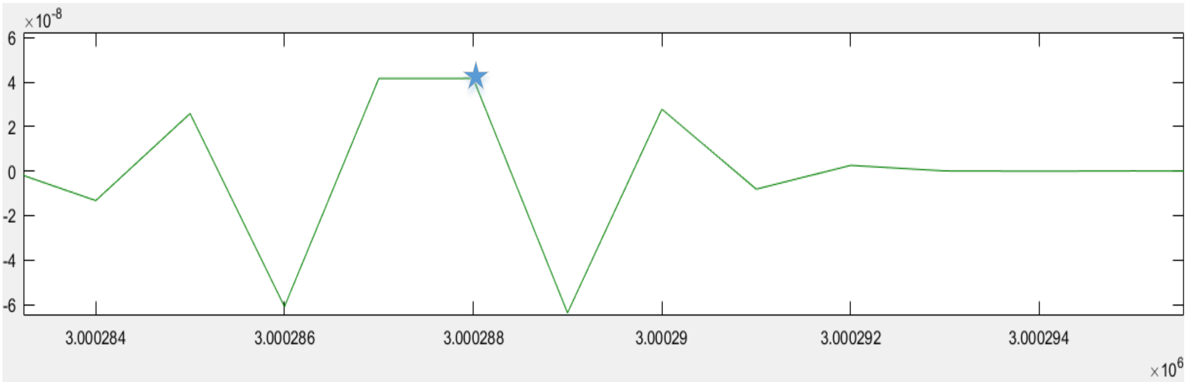

(a) Sending end arrival time of the Db6 wavelet (level 1) for a line to line fault (AB) at 0.75 km from the source

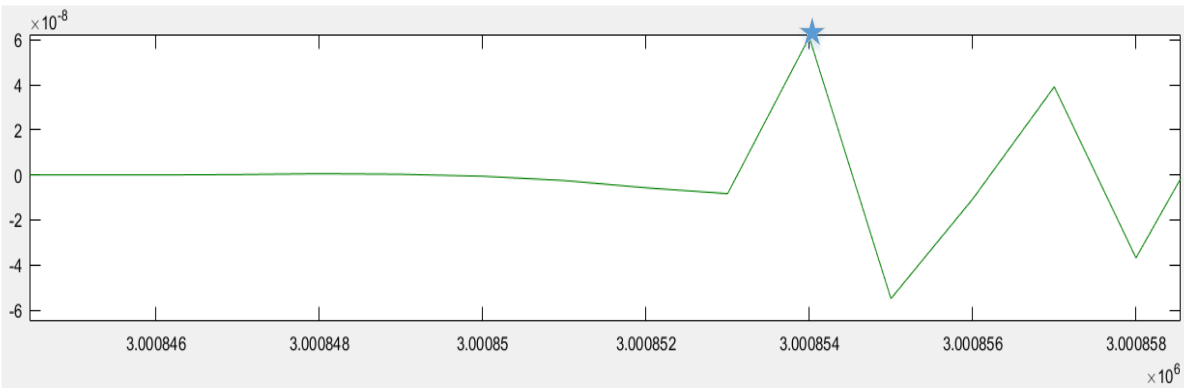

(b) Receiving end arrival time of the Db6 wavelet (level 1) for a line to line fault (AB) at 0.75 km from the source.

Figure 6 Extracting the arrival time of the detail coefficients from the Db6 wavelet (Level 1) at the sending end and the receiving end.

DOI: 10.5614/j.eng.technol.sci.2023.55.2.2

Table 2 Result for different fault distances with different fault types of the tested feeder.

Fault Type	Actual Distance	tr	ts	Estimated Distance	FDEA
AB	0.75623 km	3000288	3000854	0.753 km	99.95 %
AC	1.51246 km	3000570	3001710	1.52 km	99.90 %
BC	1.890575 km	3000003	3000712	1.87678 km	99.82 %
ABC	2.26869 km	3000854	3002561	2.27 km	99.98 %
AG	3.02492 km	3001138	3001852	0.949 km	72.55 %
BG	3.78115 km	3001423	3002314	1.18 km	65.60 %
CG	4.53738 km	3001711	3002780	1.42 km	58.77 %
ABG	5.29361 km	3001993	3003240	1.66 km	51.95 %
BCG	6.04984 km	3002276	3003414	1.51 km	39.97 %
CAG	6.80607 km	3002560	3003129	0.757 km	20.01 %
ABCG	0.75623 km	3000289	3000855	0.75623 km	99.95 %

With Karrenbauer Transformation

In condition (B), different fault types with different faulted phase currents are applied to the Karrenbauer transformation to get the alpha, beta, gamma, and zero modal components of the faulted phase currents. Instead of using the wavelet analyzer toolbox in this condition, a MATLAB script file (M file) is created to calculate the fault distance according to the procedures set out in the proposed methodology. The proposed methodology for the MATLAB script file is shown in Figure 7.

```
f=50;
wt=90;
xa=Ia_33; xb=Ib_33; xc=Ic_33; %Faulted Phase Current from MATLAB Model of Tested Feeder
Ialpha=1/3*(xa-xb); %Line Model between Phase A & B
Ibeta=1/3*(xa-xc); % Line Model between Phase A & C
Igamma=1/3*(xb-xc); % Line Model between Phase B & C
I01=1/3*(xa+xb+xc); % Zero Model
dt_max=0.3486e5;
% dt_max=0.3486e5;%according to possible maximum length from measured terminal...
                  %and sampling frequency
[cAa,cDa]=dwt(Ialpha,'db6');% Daubechies Wavelet
Aa=upcoef('aa', cAa,'db6',1,length(d7)); % Approximation Coefficient
Da=upcoef('da', cDa,'db6',1,length(d7)); % Detail Coefficient
[pa,ta]=max(abs(Da(abs(abs((abs(t01)-dt_max))):abs(t01)))); % maximum vaules of detail coefficients
ts=1e-7; %Sampling Time
l0=12.368e-3; % Zero Sequence Inductance
l1=0.4516e-3; % Positive Sequencce Inductance
c0=18.38e-9; % Zero Sequence Capacitance
c1=24.7e-9; % Positive Sequence Capacitance
v0=1/sqrt(l0*c0); % Velocity of Zero Model component of traveling wave
v1=1/sqrt(l1*c1); % Velocity of Line Model Component of traveling wave
Dt1=(t0t1-((t0t1-dt_max)+tgt1))*ts; % Time delay
x1=v0*v1*(Dt1)/((v1-v0)); %Distance
XT=[x1];
```

Figure 7 MATLAB script file for the proposed methodology.

Three different types of detail coefficient levels are used to find the fault distance:

(i) detail coefficient level 1 (D1),
(ii) combination of detail coefficient level 1+ 2 (D1+2), and
(iii) combination of detail coefficient level 1+2+3 (D1+2+3).

Figure 8 shows the MATLAB workspace results for the distance of 0.75623 km and Tables 3 to 5 show the results for the different distances tested with three different types of detail coefficients.

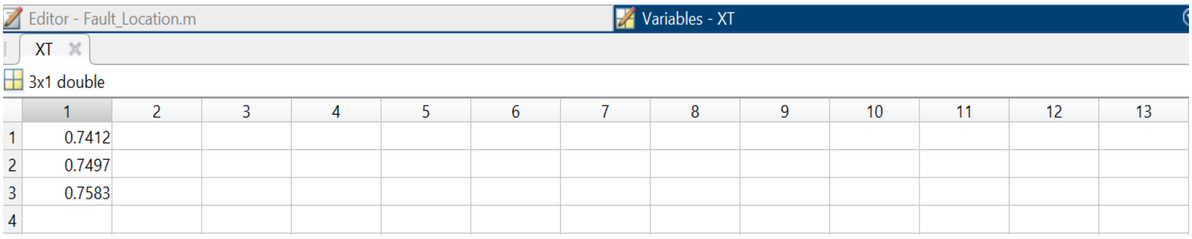

Figure 8 MATLAB workspace results for the distance of 0.75623 km tested with three different types of coefficients.

Table 3 Results for the fault distance of the tested feeder with detail coefficient level 1 (D1).

Fault Type	Actual Distance	Time Delay	Estimated Distance	FDEAC
AG	0.75623 km	8.7e-06	0.7412 km	99.80 %
BG	1.51246 km	1.77e-05	1.5079 km	99.94 %
CG	1.890575 km	2.19e-05	1.8658 km	99.67 %
AB	2.26869 km	2.66e-05	2.2662 km	99.97 %
BC	3.02492 km	3.55e-05	3.0245 km	99.99 %
AC	3.78115 km	1.583e-04	3.7742 km	99.90 %
ABG	4.53738 km	5.3e-05	4.5154 km	99.71 %
BCG	5.29361 km	6.19e-05	5.2737 km	99.99 %
ACG	6.04984 km	7.09e-05	6.0490 km	99.98%
ABC	6.80607 km	7.98e-05	6.7987 km	99.90%
ABCG	7.18418 km	9.55e-05	8.144 km	87.29 %
Average Fault Information Accuracy				98.74 %

At the first level of decomposition, the detail coefficients captured the coarsest high-frequency details of the signal. According to Table 3, detail coefficient level 1 could be utilized to analyze large-scale, general trends in the fault signal. The results show that the ground fault location could be accurately determined after applying the modal transformation to the detail coefficients at level 1.

Table 4 Results for the fault distance of the tested feeder with detail coefficient level 1+ 2 (D1+2).

Fault Type	Actual Distance	Time Delay	Estimated Distance	FDEAC
AG	0.75623 km	8.8e-06	0.7497 km	99.91 %
BG	1.51246 km	1.78e-05	1.5165 km	99.94 %
CG	1.890575 km	2.21e-05	1.8828 km	99.89 %
AB	2.26869 km	2.64e-05	2.2492 km	99.74 %
BC	3.02492 km	3.54e-05	3.0159 km	99.88 %
AC	3.78115 km	1.583e-04	3.7742 km	99.90 %
ABG	4.53738 km	5.31e-05	4.5239 km	99.82 %
BCG	5.29361 km	6.19e-05	5.2737 km	99.99 %
ACG	6.04984 km	7.09e-05	6.0405 km	99.87 %
ABC	6.80607 km	7.98e-05	6.7987 km	99.90%
ABCG	7.18418 km	9.31e-05	7.9318 km	90.11 %
Average Fault Information Accuracy				98.99%

The detail coefficients at level 2 captured finer high-frequency details that were not captured at level 1. By combining two sets of detail coefficients (level 1+2), a more comprehensive analysis of the high-frequency components of the signal could be obtained. After applying the modal transformation to the combination of detail coefficients at levels 1 and 2, Table 4 shows that accurate fault location could be determined for all types of faults.

Detail coefficients at level 3 captured finer high-frequency details than the previous level 1 and 2. Combining detail coefficient levels 1, 2, and 3 involves using the detail coefficients at all three levels to analyze the signal. Additionally, using all three detail coefficient levels could improve the accuracy of the feature extraction

DOI: 10.5614/j.eng.technol.sci.2023.55.2.2

algorithm by providing a more detailed representation of the signal. Table 5 shows the results for the fault distance of the tested feeder with detail coefficient level 1+2+3 (D1+2+3).

Table 5 Results for the fault distance of tested feeder with detail coefficient level 1+2+3 (D1+2+3)

Fault Type	Actual Distance	Time Delay	Estimated Distance	Error
AG	0.75623 km	8.9e-06	0.7583 km	99.97 %
BG	1.51246 km	1.75e-05	1.4909 km	99.71 %
CG	1.890575 km	2.21e-05	1.8828 km	99.89 %
AB	2.26869 km	2.65e-05	2.2577 km	99.86 %
BC	3.02492 km	3.55e-05	3.0245 km	99.99 %
AC	3.78115 km	1.583e-04	3.7742 km	99.90 %
ABG	4.53738 km	5.31e-05	4.5239 km	99.82 %
BCG	5.29361 km	6.21e-05	5.2907 km	99.77 %
ACG	6.04984 km	7.11e-05	6.0575 km	99.89 %
ABC	6.80607 km	7.98e-05	6.8072 km	99.98 %
ABCG	7.18418 km	8.41e-05	7.1651 km	99.74%
Average Fault Information Accuracy				99.86 %

According to the results shown in Table 3 to 5, the proposed method followed by the Karrenbauer transformation gives higher accuracy for the estimation of fault distance. The tested feeder was tested in three detail coefficient conditions: detail coefficient level 1 (D1) with a fault distance estimation accuracy (FDEA) of over 99% and an average fault information accuracy (AFIA) of 98.74%; and detail coefficient level 1+2 (D1+2) with an FDEA of over 99% and an AFIA of 98.99%. The combination of detail coefficient level 1+2+3 (D1+2+3) gave the highest accuracy for estimation of the fault distance compared to the other two conditions, with an FDA of over 99% and an AFIA of 99.86%.

Conclusion

This paper presented the estimation of fault distance in radial distribution networks with signal processing techniques. Although signal-processing techniques are applied to fault location techniques, the fault distance cannot be detected accurately without the use of modal transformation. The proposed methodology uses the Karrenbauer modal transformation of faulted phase currents and after that the signal processing techniques are applied. The advantage of modal transformation is that it can reduce the mutual effects of inductive coupling of the line and prevent interference from other power lines. Among the signal processing techniques, the wavelet transform with multi-level decomposition is applied to extract fault feature conditions. The results indicated that the combination of detail coefficient level 1+2+3 (D1+2+3) gave the highest accuracy for the estimation of the fault distance. Therefore, the proposed methodology is very efficient and has high accuracy in estimating fault distance in radial distribution networks.

References

[1] Lee, S.J., Choi, M.S., Kang, S.H., Jin, B.G., Lee, D.S., Ahn, B.S., Yoon, N.S., Kim, H.Y. & Wee, S.B., *An Intelligent and Efficient Fault Location and Diagnosis Scheme for Radial Distribution Systems*, IEEE Transactions on Power Delivery**, 19**(2), pp. 524-532, April 2004.

[2] Ngu, E.E. & Ramar, K.*, A Combined Impedance and Traveling Wave based Fault Location Method for Multi-Terminal Transmission Lines*, Electrical Power and Energy System, **33**(10), pp. 1767-1775, 2011. doi: 10.1016/j.ijepes.2011.08.020.

[3] Sadeh, J., Bakhshizadeh, E. & Kazemzadeh, R., *A New Fault Location Algorithm for Radial Distribution Systems Using Modal Analysis*, Electrical Power and Energy System, **45**(1), pp. 271-278, 2013. doi: 10.1016/j.ijepes.2012.08.053.

[4] Jiao, X. & Liao, Y., *Accurate Fault Location for Untransposed/Transposed Transmission Lines Using Sparse Wide-Area Measurements*, IEEE Transactions on Power Delivery, **31**(4), pp. 1797-1805, August 2016.

[5] Shi, S., Lei, A., He, X., Mirsaeidi, S. & Dong, X., *Travelling Waves-based Fault Location Scheme for Feeders in Power Distribution Network*, The Journal of Engineering, **2018**(15), 2018.

[6] Hasanvand, H., Soleymani, S., Feizifar, B. & Zad, B.B., *Fault Location in Distribution Networks using S-Transform*, Journal of Electrical Engineering, **14**(1), pp. 371-375, January 2014.
[7] da Silva, P.R.N., Negrão, M.M.L., Junior, P.V. & Sanz-Bobi, M.A., *A New Methodology of Fault Location for Predictive Maintenance of Transmission Lines*, Electrical Power and Energy Systems, pp. 568-574, 2012.
[8] Apostolopoulos, C.A. & Korres, G.N., *Accurate Fault Location Algorithm for Double-Circuit Series Compensated Lines Using a Limited Number of Two-End Synchronized Measurements*, Electrical Power and Energy System, pp. 495-207, 2012.
[9] Sadeh, J., Bakhshizadeh, E. & Kazemzadeh, R., *New Fault Location Algorithm for Radial Distribution Systems Using Modal Analysis*, Electrical Power and Energy System, **45**(1), pp. 271-278, 2013.
[10] Evrenosoglu, C.Y. & Abur, A., *Fault location in Distribution Systems with Distributed Generation*, In: 15th Power system computation conference (PSCC'05), Liege, Belgium, August 2005.
[11] Nouri, H., Wang, C. & Davies, T., *An Accurate Fault Location Technique for Distribution Lines with Tapped Loads Using Wavelet Transform*, in: Proc IEEE Power Tech Porto, pp. 10-133, September 2001.
[12] Magnago, F.H. & Abur, A., *A New Fault Location Technique for Radial Distribution Systems Based on High Frequency Signals*, IEEE Power Eng Soc 1999; 1:426–31, 18–22 July 1999.
[13] Hidayatullah, F.A. & Husein, A., *Self-Potential Method to Assess Embankment Stability: A Study Related to the Sidoarjo Mud Flow*, Journal of Engineering and Technological Sciences, **52**(5), pp. 707-731. 2020.
[14] Yadav, A.R., Anand, R.S., Dewal, M.L. & Gupta, S., *Performance Analysis of Discrete Wavelet Transform Based First-Order Statistical Texture Features for Hardwood Species Classification*, 3rd International Conference on Recent Trends in Computing 2015 (ICRTC-2015), pp. 214-221, 2015.
[15] Neelov, A.I. & Goedecker, S., *An Efficient Numerical Quadrature for the Calculation of the Potential Energy of Wavefunctions Expressed in the Daubechies Wavelet Basis*, Journal of Computational Physics, **217**(2) pp. 312-339, 2006.

Manuscript Received: 12 December 2022
Revised Manuscript Received: 15 April 2023
Accepted Manuscript: 27 April 2023